


ORIGINAL RESEARCH

Open Access



Impact of cognitive impairment on heart failure prognosis: insights into central nervous system mechanism

Zhiyong Shi^{1†}, Mingkai Yun^{1†}, Binbin Nie², Enjun Zhu³, Wei Fu³, Baoci Shan², Sijin Li⁴, Xiaoli Zhang^{1*}  and Xiang Li^{5,6}

Abstract

Background Epidemiological studies have indicated that patients with heart failure (HF) who experience cognitive impairment (CI) have a poor prognosis. While poor self-management and compliance are suggested as contributing factors, they do not fully explain the underlying mechanisms of high risk of cardiac events in HF patients with CI. Given the interconnectedness of CI and the autonomic nervous system (ANS), both regulated by the central nervous system, this study investigated the relationship among cognitive function, metabolism in ANS-related brain regions, and major arrhythmic events (MAEs) in patients with HF with reduced ejection fraction (HFrEF).

Results We retrospectively enrolled 72 patients with HFrEF who underwent gated myocardial perfusion imaging, heart and brain ¹⁸F-FDG positron emission tomography/computed tomography imaging, and cognitive testing. Cognitive function was evaluated using the Mini-Mental State Examination. During the follow-up period, 13 patients (17.8%) experienced MAEs. Patients with MAEs exhibited decreased cognitive function across various domains, including orientation, registration, and language and praxis (all $p < 0.05$). Patients with CI displayed a prolonged heart rate-corrected QT (QTc) interval and hypometabolism in the left hippocampus and bilateral caudate nuclei (all $p < 0.05$). Significant correlations were observed between cognitive function, QTc interval, and metabolism in ANS-related brain regions (all $p < 0.05$). Cox regression model analysis showed that the predictive value of cognitive function is not independent of the QTc interval and there is a significant interaction. The mediation analyses suggested that a prolonged QTc interval resulting from ANS disorder increased risk of MAEs in HFrEF patients with CI. Patients with CI exhibited reduced central autonomic network (CAN) connectivity.

Conclusion ANS dysfunction, exacerbated by reduced metabolism in ANS-related brain regions and CAN connectivity, contributed to an increased risk of MAEs in HFrEF patients with CI.

Keywords ¹⁸F-FDG PET, Cognitive impairment, Brain–heart axis, QTc interval, Brain network, Heart failure

[†]Zhiyong Shi and Mingkai Yun have equally contributed to this work.

*Correspondence:

Xiaoli Zhang

xlzhang68@126.com

Full list of author information is available at the end of the article



Background

Heart failure (HF) is a life-threatening syndrome characterized by multifaceted aspects, and its global incidence and mortality rates are rising due to population aging and increasing cardiovascular risk factors [1]. The physical and mental well-being of patients with HF typically deteriorates, often resulting in cognitive impairment (CI) and dysfunction in the autonomic nervous system (ANS). CI is strongly associated with ANS dysfunction [2–5], and the latter may occur earlier [6]. HF patients with CI often have a worse prognosis, which is potentially linked to decreased self-care and compliance [7]. However, this alone does not fully explain the mechanisms underlying poor prognosis in HF patients with CI.

Reduced cardiac output, vascular dysfunction, and sympathetic-vagal imbalance can lead to a decline in brain function, possibly contributing to CI [8]. Additionally, ANS disorder, characterized by sympathetic overactivity and parasympathetic withdrawal, is a hallmark of HF and plays a crucial role in pathogenesis of arrhythmias [9, 10]. A prolonged heart rate-corrected QT (QTc) interval is closely related to sympathetic nerve activation and is considered an important risk factor for fatal arrhythmias and sudden cardiac death [11]. Central autonomic network (CAN) dysfunction may be a common mechanism in CI and ANS disorder [12]. The CAN is a complex network composed of a series of brain regions essential for cognition and regulation of the ANS [5, 12–14]. Core components of the CAN include the prefrontal cortex, hippocampus, hypothalamus, caudate nucleus, amygdala, dorsal vagal complex in the brainstem, and spinal cord, which are interconnected through neural pathways and collectively involved in regulating ANS functions such as heart rate, blood pressure, respiration, and digestion [15–17]. The prefrontal cortex, particularly the anterior cingulate and orbitofrontal cortices, plays a crucial role in regulating emotions, attention, and higher cognitive functions associated with ANS activity [18]. These regions influence the hypothalamus and the autonomic control centre in the brainstem through descending projections, thereby modulating heart rate and blood pressure [19].

Previous studies have shown that a reduction in regional grey matter in patients with HF, especially in the cingulate gyrus, hippocampus, and thalamus, leads to CI [20–22]. The hippocampus, vital for memory processing, along with neighbouring structures such as the cingulate gyrus, parahippocampal gyrus, and thalamus, forms the Papez circuit, which is crucial for information transmission [23, 24]. Additionally, our previous study demonstrated that, even after adjusting for traditional arrhythmogenic risk factors, metabolism in ANS-related brain regions—including the insula, hippocampus,

cingulate gyrus, caudate nucleus, and thalamus—was a significant independent predictor of major arrhythmic events [25]. ANS dysfunction may increase the risk of ventricular arrhythmias (VA) and sudden cardiac death by exacerbating left ventricular (LV) electrical instability [26]. However, in patients with HF, the underlying mechanisms of CI, functional impairment in specific ANS-related brain regions, and adverse outcomes, particularly VA, remain unclear. Building on existing research, this study aims to further explore the potential mechanisms underlying the poor prognosis of HF with reduced ejection fraction (HFrEF) in patients with clinically determined CI, by evaluating the potential associations among cognitive function, ANS-related neural metabolism, and LV electrical instability.

This study hypothesized that CI and ANS disorders are two clinical manifestations resulting from reduced metabolism and connectivity within the CAN in patients with HFrEF, and that the association between CI and poor prognosis may partly result from ANS disorder caused by CAN injury. Numerous studies have shown that reduced regional brain metabolism, as quantified by ^{18}F -fluorodeoxyglucose (FDG) positron emission tomography (PET)/computed tomography (CT), is closely associated with cognitive impairment [27, 28]. Therefore, this study investigated the associations among CI, CAN dysfunction, and major arrhythmic events (MAEs), as well as the potential mechanisms underlying poor prognosis in patients with HFrEF using ^{18}F -FDG PET/CT imaging.

Methods

Study population

This single-centre, retrospective, longitudinal, observational imaging study enrolled patients who underwent clinically indicated $^{99\text{m}}\text{Tc}$ -sestamibi single-photon emission computed tomography (SPECT)/CT gated myocardial perfusion imaging (GMPI) at the Beijing Anzhen Hospital between January 2018 and December 2021. A total of 87 patients underwent brain ^{18}F -FDG PET/CT scanning and cognitive testing. The inclusion criteria were chronic ischemic HF with left ventricular ejection fraction (LVEF) < 40%, absence of cerebrovascular accidents, no recent revascularization (defined as less than 3 months for percutaneous coronary intervention or less than 6 months for coronary artery bypass grafting), no history of psychiatric illness, and no evidence of substance or alcohol abuse. Details of the inclusion criteria are illustrated in Supplementary Fig. 1.

Patients with cerebral infarction detected on ^{18}F -FDG PET/CT images, those with insufficient image quality for analysis, and those missing follow-up information were excluded ($n = 15$).

An ischemic HF diagnosis was based on comprehensive clinical judgment following clinical guidelines. Ultimately, 72 patients were included in this study (Supplementary Fig. 1). All patients underwent standardized evaluations, including laboratory tests and clinical assessment [29]. The resting QTc interval was calculated using the Bazett formula.

The study protocol was approved by the Ethics Committee of the Beijing Anzhen Hospital of Capital Medical University (No. 2017024) and adhered to the principles of the Declaration of Helsinki. Written informed consent was obtained from all the participants. Two experienced nuclear cardiologists independently reviewed all images while blinded to the clinical information.

Imaging and analysis

99mTc-stemambi SPECT/CT GMPI and cardiac 18F-FDG PET/CT imaging

The SPECT/CT GMPI procedure at rest was performed as previously described [30]. Data were analysed using QGS software (version 3.1; Cedars-Sinai Medical Center) on a Siemens e.soft workstation (Siemens AG 2015) to compute the LVEF (%) and LV mechanical synchrony parameters, including bandwidth (BW, °), standard deviation (SD, °), and entropy (%) [31]. Subsequently, patient preparation followed the 2016 ASCN guidelines for PET imaging [32]. Accordingly, 370–500 MBq of ¹⁸F-FDG was injected, and data were acquired within 1 h. Myocardial perfusion and metabolic activity were analysed using the American Heart Association 17-segment and 5-point scoring system [33]. Total perfusion deficit (TPD, %LV) was derived from hypoperfusion segments. Hibernating myocardium in a perfusion defect was defined by a mismatch score of ≥ 1 , while scarring was defined by a mismatch score of < 1 . Each segment represented 6% of the LV. The extent of hibernating myocardium and scarring (%LV) was calculated based on mismatched or matched segments.

Brain ¹⁸F-FDG PET/CT

Brain ¹⁸F-FDG PET/CT imaging was conducted in accordance with the guidelines of the European Society of Nuclear Medicine [34]. Participants were positioned in a comfortable and tranquil room with subdued lighting. One hour after the injection, 3D images of the brain using ¹⁸F-FDG were captured for 10 min using a high-resolution PET scanner (Biograph mCT, Siemens Healthcare). These images were reconstructed using 5 iterations and 21 subsets to achieve a high spatial resolution. In addition, CT transmission scan (120 kV, 240 mAs) was used for attenuation correction. To quantify regional brain metabolic activity, a validated methodology was employed. In brief, the preprocessing of cerebral PET/CT

images utilized SPM12 (Wellcome Department of Cognitive Neurology, London, UK). Initially, all cerebral FDG PET scans were normalized to the Montreal Neurological Institute (MNI) space and resampled to $2 \times 2 \times 2$ mm³ voxels. These normalized images were then smoothed using an 8 mm³ full width at half maximum (FWHM) Gaussian kernel. Subsequently, intracranial tissues were extracted from the smoothed images using a brain mask image in MNI space. Regions of interest were identified in MNI space using automated anatomical labelling (AAL) atlases, and the standardized uptake values (SUVmean) of the left and right brain regions were determined. The standardized uptake value ratio was calculated by dividing the SUVmean in each brain region by the SUVmean in the cerebellum. Following these procedures, researchers were able to accurately assess and quantify the regional brain metabolic activity in patients with HF/EF undergoing ¹⁸F-FDG PET/CT imaging. To construct the metabolic CAN, 16 nodes (8 nodes per hemisphere) associated with the parasympathetic nervous system and 20 nodes (10 nodes per hemisphere) linked to the sympathetic nervous system were selected from the AAL atlas. This atlas has been previously utilized in imaging-based studies to assess central autonomic processing in humans [17, 35]. Pearson's correlation coefficients between each pair of regions of interest were computed in an inter-subject manner to define the network edges. Subsequently, two weighted network matrices (16×16 and 20×20) were created for each subgroup. The networks of patients with and without CI were then statistically compared using a permutation test. The metabolic brain networks were visualized using the BrainNet Viewer software [25].

Cognitive function tests

To further investigate the impact of CI, we conducted cognitive function tests with the patients. Specifically, 77 patients completed the Mini-Mental State Examination (MMSE), where scores of ≤ 26 indicated CI.

Endpoints and follow-up

The primary endpoints were MAEs, including sustained ventricular tachycardia with hemodynamic compromise, sudden cardiac death, cardiac arrest, and appropriate implantable cardioverter-defibrillator therapy. Events were adjudicated by physicians blinded to the SPECT and PET data and confirmed through a combination of medical records, clinical visits, and telephone interviews. In cases of multiple MAEs, the earliest event was recorded. All-cause death was considered the secondary outcome.

Statistical analyses

Data analyses were performed using SPSS software (version 22.0; Armonk, NY, USA) and R 4.2.0 (R Foundation

for Statistical Computing, Vienna, Austria). Categorical data were presented as counts and percentages (%), while continuous variables were expressed as mean \pm SD or median with interquartile range (IQR). Normality was assessed using the Kolmogorov–Smirnov test. Student's *t*-test was used to compare normally distributed variables, whereas the Kruskal–Wallis and Mann–Whitney *U* tests were used to examine non-normally distributed variables. Chi-squared or Fisher's exact tests were used to compare categorical data. Pearson's or Spearman's coefficients were employed to evaluate correlations. Kaplan–Meier curves were used to depict event occurrence time data, with survival rates compared using the log-rank test. Cox proportional hazard models were used to calculate the hazard ratios (HR) and 95% confidence intervals after adjusting for covariates. The residual analysis method was used to explore the impact of CI on metabolic levels while controlling for inter-individual differences in cognitive function. First, a linear regression model was constructed, with MMSE score and PET metabolic level as the independent and dependent variables, respectively, to fit an individual's metabolic level. Subsequently, residuals were extracted from this model, representing the variation in metabolic level after controlling for the influence of the MMSE score. An independent samples *t*-test was used to compare the differences in residuals between the CI and non-CI groups to evaluate the differences in neurometabolism and QTc interval between the two groups after controlling for the influence of the MMSE score. Welch's test was used for the *t*-test to handle possible issues of unequal variances. The net reclassification improvement (NRI) method was used to conduct a formal risk reclassification analysis. A multivariable stepwise linear regression analysis was performed, adjusting for sex, age, hyperlipidaemia, hypertension, diabetes, and body mass index (BMI), to evaluate the relationship among cognitive function, metabolism in ANS-related brain regions, and the QTc interval. Mediation analysis was conducted to assess the impact of ANS-related neural metabolism on MAEs via LV electrical instability. Permutation tests assessed the statistical significance of the network differences (family-wise error [FWE]-corrected 5000 times). A *P*-value of <0.05 was considered statistically significant. Notably, the *P*-values were not adjusted for multiplicity, which may have affected the reproducibility of statistical inferences.

Results

Study population

The final study cohort comprised 72 patients with HFrEF, with a median age of 57 ± 10 years and predominantly men (91.7%). Table 1 summarizes the demographic, clinical, and laboratory characteristics of the patients. Among

the 72 patients, 30 (41.7%) were categorized with New York Heart Association functional class III or IV, and 61 (84.7%) were prescribed beta-blockers.

As shown in Table 1, patients who experienced MAEs exhibited a prolonged QTc interval and reduced LVEF compared to patients without MAEs. No significant differences were observed in the LV dimensions (end-diastolic and end-systolic volumes) or LV mechanical synchrony parameters (BW, SD, and entropy) between patients with and without MAEs (all $p > 0.05$). Similarly, there were no statistically significant differences in cardiovascular risk factors (hypertension, diabetes, hyperlipidaemia, smoking history, and family history) between the two groups (all $p > 0.05$). Moreover, there were no notable differences in medication use between the two groups (all $p > 0.05$).

Outcome

The median follow-up period was 2.4 years (IQR: 1.0–3.6 years). MAEs occurred in 13 (18.1%) patients. The univariate analysis identified the risk factors associated with MAEs (Supplementary Table 1). Kaplan–Meier survival analysis stratified the entire cohort into two groups based on CI status, revealing a significantly reduced survival rate in patients with CI compared to those without CI (61.5% vs. 8.5%, HR_{adj} : 7.145 [95% confidence interval: 1.543–33.089]; $p < 0.001$; Fig. 1). The relationship between cognitive function and MAEs remained significant after multivariable adjustment for traditional cardiovascular risk factors (Table 2).

During follow-up, 13 patients (18.1%) experienced the secondary endpoint of all-cause death. Patients with CI exhibited a significantly higher incidence of all-cause death compared to those without CI (30.8% vs. 8.5%, HR_{adj} : 4.531 [95% confidence interval: 1.044–19.676]; $P = 0.047$; Supplementary Fig. 2). Cognitive function as a continuous variable, corrected for age, sex, LVEF, and arrhythmia history, remained an independent predictor of all-cause mortality in patients with HFrEF (HR_{adj} : 0.721 [95% confidence interval: 0.531–0.979]; $P = 0.036$; Supplementary Table 2).

LV electrical instability and ANS-related neurometabolic status in patients with CI

Patients with CI exhibited significantly lower metabolic activity in the left hippocampus and bilateral caudate nucleus compared to those without CI (0.72 ± 0.08 vs. 0.75 ± 0.05 , $P = 0.035$; 0.81 ± 0.11 vs. 0.70 ± 0.16 , $P = 0.004$; 0.66 ± 0.11 vs. 0.56 ± 0.12 , $P = 0.005$; Fig. 2). In addition, critical differences were observed in metabolic activity in the left anterior cingulate gyrus (1.08 ± 0.10 vs. 1.02 ± 0.08 , $P = 0.061$), left superior parietal gyrus (1.15 ± 0.11 vs. 1.08 ± 0.14 , $P = 0.079$);

Table 1 Baseline characteristics of study participants according to MAEs

	All patients (n = 72)	Patients without MAEs (n = 59)	Patients with MAEs (n = 13)	P Value
Age, years, mean ± SD	56.8 ± 10.3	56.3 ± 10.8	58.9 ± 8.0	0.428
Male, n (%)	66 (91.7)	53 (89.8)	13 (100)	0.583
BMI, kg/m ² , mean ± SD	25.7 ± 3.1	25.8 ± 3.3	25.2 ± 2.1	0.585
Heart rate, b.p.m (IQR)	76.5 (70.0, 85.0)	76.0 (70.0, 83.5)	78.5 (70.5, 87.3)	0.624
SBP, mmHg, (IQR)	121.5 (106.8, 130.0)	120.5 (107.5, 130.0)	129.0 (106.3, 130.0)	0.701
QTc interval, ms, mean ± SD	448.3 ± 27.3	443.0 ± 24.6	472.9 ± 26.8	0.001
Hypertension, n (%)	45 (62.5)	37 (62.7)	8 (61.5)	1.000
Diabetes, n (%)	33 (45.8)	25 (42.4)	8 (61.5)	0.235
Hyperlipidemia, n (%)	38 (52.8)	29 (49.2)	9 (69.2)	0.231
Smoker, n (%)	41 (56.9)	32 (54.2)	9 (69.2)	0.371
Family history of CAD, n (%)	23 (31.9)	22 (37.3)	1 (7.7)	0.050
Prior arrhythmia, n (%)	9 (12.5)	6 (10.2)	3 (23.1)	0.349
NYHA				0.130
I-II, n (%)	42 (58.3)	37 (62.7)	5 (38.5)	
III-IV, n (%)	30 (41.7)	22 (37.3)	8 (61.5)	
Serum biomarkers				
Triglycerides, mmol/L, (IQR)	1.4 (1.1, 1.9)	1.4 (1.1, 1.9)	1.2 (0.8, 1.6)	0.133
hsCRP, mg/L, (IQR)	1.5 (0.7, 3.8)	1.5 (0.6, 3.5)	1.4 (1.1, 6.7)	0.261
BNP, pg/mL, (IQR)	267.5 (126.3, 418.3)	215.5 (110.8, 386.5)	387.0 (182.3, 662.0)	0.072
eGFR, ml/min/1.73m ² , (IQR)	93.0 (82.2, 101.7)	92.3 (83.7, 101.7)	96.3 (80.6, 101.5)	0.957
Serum albumin, g/L, mean ± SD	43.5 ± 2.9	43.9 ± 2.9	42.2 ± 2.4	0.060
Creatinine, μmol/L, (IQR)	81.2 (70.9, 91.3)	81.0 (71.3, 91.5)	81.9 (67.4, 92.9)	0.941
Medication				
Beta-blocker, n (%)	61 (84.7)	49 (83.1)	12 (92.3)	0.676
ARNI/ACE inhibitors/ARBs, n (%)	52 (72.2)	43 (72.9)	9 (69.2)	0.746
Spirolactone, n (%)	41 (56.9)	35 (59.3)	6 (46.2)	0.538
Aspirin, n (%)	61 (84.7)	49 (83.1)	12 (92.3)	0.676
Digoxin, n (%)	5 (6.9)	4 (6.8)	1 (7.7)	1.000
Imaging parameters				
TPD, %/LV, mean ± SD	43.1 ± 14.8	42.9 ± 14.0	44.0 ± 18.6	0.819
HM, %LV, (IQR)	15.0 (8.0, 25.8)	14.0 (8.0, 26.0)	18.0 (0.0, 27.0)	0.814
Scar burden, %LV, mean ± SD	25.3 ± 16.9	24.9 ± 16.1	27.5 ± 20.7	0.622
EDV, mL, (IQR)	188.0 (150.0, 260.8)	188.0 (149.0, 257.0)	207.0 (160.0, 272.0)	0.578
ESV, mL, (IQR)	150.0 (112.8, 209.8)	147.0 (108.0, 203.0)	174.0 (131.5, 230.0)	0.269
LVEF, %, mean ± SD	21.8 ± 6.9	22.6 ± 6.7	17.9 ± 6.4	0.025
Phase BW, °, mean ± SD	125.2 ± 38.9	123.6 ± 40.1	132.0 ± 33.6	0.488
Phase SD, °, mean ± SD	34.2 ± 11.4	33.3 ± 11.5	38.3 ± 10.0	0.151
Entropy, %, mean ± SD	67.7 ± 6.8	67.3 ± 6.8	69.5 ± 7.2	0.312

Values are median (25th, 75th), n (%), or mean ± SD. No corrections for multiple testing were applied. ACE = angiotensin-converting enzyme; ARB = angiotensin receptor blocker; ARNI = angiotensin receptor neprilysin inhibitor; BNP = brain natriuretic peptide; BMI = body mass index; BW = bandwidth; EDV = end diastolic volume; eGFR = estimated glomerular filtration rate; ESV = end systolic diastolic volume; HM = hibernating myocardium; HMA = Hippocampal metabolic activity; hs-CRP = high-sensitivity C-reactive protein; LVEF = left ventricular ejection fraction; MAEs = major arrhythmic events; MMSE = minimum mental state examination; NYHA = New York Heart Association; QTc = corrected QT; SUVR = standardized uptake values ratio; TPD = total perfusion deficit.

and left thalamus (1.10 ± 0.09 vs. 1.05 ± 0.13 , $P = 0.099$) between those with and without CI. As shown in Fig. 3A, the QTc interval was significantly prolonged in patients with CI compared to that in those without CI (473.2 ± 27.7 ms vs. 442.4 ± 23.8 ms, $p < 0.001$).

To investigate the impacts of CI on neurometabolism and QTc intervals while accounting for individual differences in cognitive function, residual analysis was employed to compare the disparities in ANS-related neurometabolism and QTc intervals between the CI

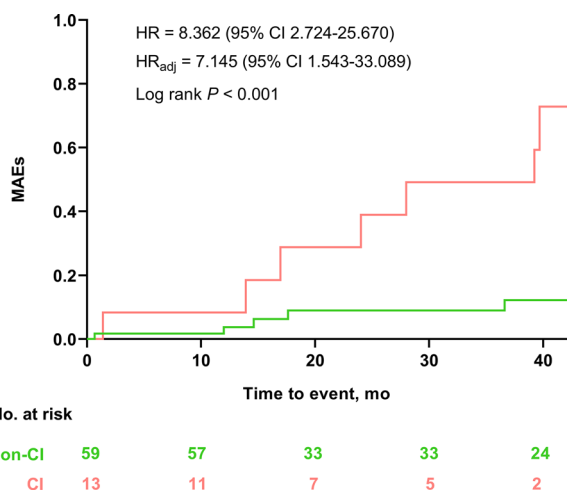


Fig. 1 Kaplan–Meier survival curves of MAEs. The incidence of MAEs in the CI group was significantly higher than that in the non-CI group. Adjusted covariables included age, sex, LVEF, and arrhythmia history. CI = cognitive impairment; MAEs = major arrhythmic events; HR_{adj} = adjusted hazard ratio

Table 2 Univariate and multivariate analysis of cognitive function vs MAEs in patients with HFrEF

	Cognitive function	
	HR (95% CI)	P Value
Univariate		
Per unit change	0.639 (0.526–0.777)	< 0.001
Per SD change	0.404 (0.272, 0.600)	< 0.001
Covariates: age and sex		
Per unit change	0.639 (0.523–0.781)	< 0.001
Per SD change	0.404 (0.269–0.605)	< 0.001
Covariates: scar burden and LVEF		
Per unit change	0.608 (0.486–0.761)	< 0.001
Per SD change	0.366 (0.232, 0.576)	< 0.001
Covariates: HM and revascularization		
Per unit change	0.647 (0.523–0.801)	< 0.001
Per SD change	0.414 (0.269, 0.638)	< 0.001
Covariates: combined cardiac risk factors ^a		
Per unit change	0.541 (0.385–0.759)	< 0.001
Per SD change	0.288 (0.145, 0.572)	< 0.001

BNP = brain natriuretic peptide; CI = confidence interval; HM = hibernating myocardium; HR = hazard ratio; LVEF = left ventricular ejection fraction; MAEs = major arrhythmic events; TPD = total perfusion deficit.

^a The cardiac risk factors that were included in this model were each of the cardiovascular risk factors ($P < 0.1$) that were significantly associated with the development of events based on the univariate analysis (Table S1)—family history, serum albumin, and BNP—that were included as cofactors in a stepwise (forward) conditional manner

and non-CI groups. Furthermore, patients with MAEs showed significantly lower metabolism in most ANS-related brain regions compared to those without MAEs (all $p < 0.05$), as shown in Supplementary Fig. 3. After controlling for cognitive function, only the metabolic activity of the left caudate nucleus showed a statistically significant difference between the MAEs and non-MAEs groups (all $p < 0.05$; Supplementary Table 4).

Correlations among cognitive function, LV electrical instability, and ANS-related brain region metabolism

Our findings revealed a significant correlation between cognitive function and the QTc interval ($r = -0.429$, $P = 0.001$; Fig. 3B). As shown in Supplementary Fig. 4 and Supplementary Table 5, there were significant correlations among cognitive function and neurometabolism in the insula, anterior cingulate gyrus, hippocampus, caudate nucleus, thalamus, and superior temporal gyrus (all $p < 0.05$). Significant correlations were also observed between QTc and neurometabolism in the dorsolateral superior frontal gyrus, medial superior frontal gyrus, insula, anterior cingulate gyrus, hippocampus, amygdala, superior parietal gyrus, supramarginal gyrus, precuneus, caudate nucleus, pallidum, thalamus, and superior temporal gyrus (all $p < 0.05$). After correction for cognitive function, the QTc interval remained significantly related to neurometabolism in the hippocampus, supramarginal gyrus, caudate nucleus, pallidum, thalamus, and superior temporal gyrus (all $p < 0.05$; Supplementary Tables 6). Figure 4 and Supplementary Tables 7 present the correlations among bilateral ANS-related neurometabolic activities, QTc interval, and cognitive function. Significant correlations were found between cognitive function and neurometabolic activities in the right insula, right anterior cingulate gyrus, bilateral hippocampus, left amygdala, bilateral thalamus, and left superior temporal gyrus (all $p < 0.05$). Additionally, significant correlations were found between the QTc interval and neurometabolism in the bilateral medial superior frontal gyrus, bilateral insula, bilateral anterior cingulate gyrus, bilateral hippocampus, left amygdala, left superior parietal gyrus, bilateral supramarginal gyrus, bilateral caudate nucleus, bilateral pallidum, bilateral thalamus, and bilateral superior temporal gyrus (all $p < 0.05$). After correcting for cognitive function, the QTc interval was closely related to neurometabolism in the bilateral insula, bilateral hippocampus, left amygdala, bilateral caudate nucleus, bilateral pallidum, right thalamus, and bilateral superior temporal gyrus (all $p < 0.05$; Supplementary Tables 8). Notably, ANS-related neurometabolic activity was not associated with LVEF in patients with HFrEF (all $p > 0.05$; Supplementary Tables 5 and 7).

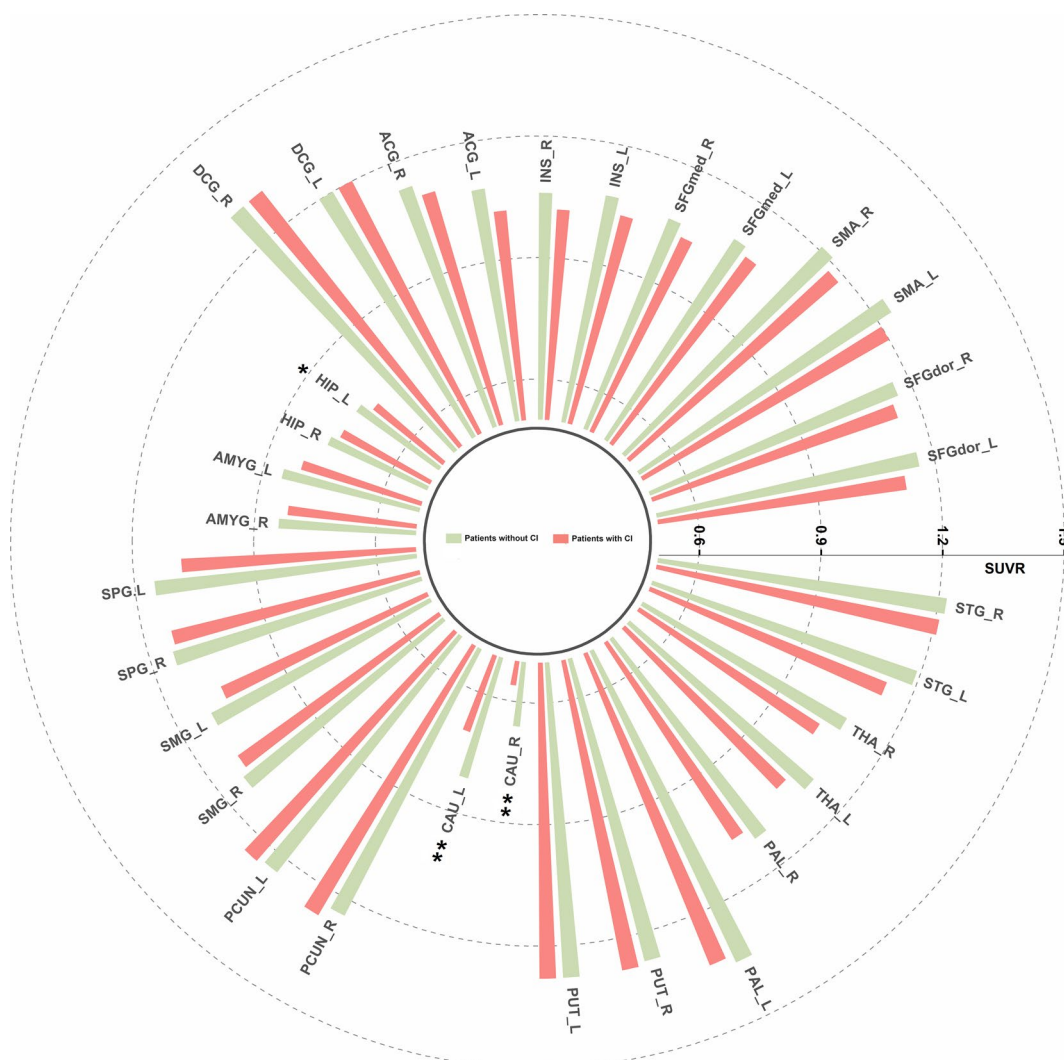


Fig. 2 Comparative analysis of ANS-related neurometabolic activity in patients with and without CI. Patients with CI had significantly reduced metabolic activity in the left hippocampus and bilateral pallidum. ACG=anterior cingulate gyrus; AMYG=amygdala; ANS=autonomic nervous system; CAU=caudate nucleus; CI=cognitive impairment; DCG=median cingulate and paracingulate gyri; HIP=hippocampus; INS=insula; L=left; PCUN=Precuneus; PUT=putamen; R=right; SFGdor=superior frontal gyrus, dorsolateral; SFGmed=superior frontal gyrus, medial; SMA=supplementary motor area; SMG=supramarginal gyrus; SPG=Superior parietal gyrus; STG=superior temporal gyrus; THA=thalamus

Prognostic value of CI/ANS-related brain regions metabolism on QTc interval

We conducted stepwise linear regression analysis with the QTc interval as the dependent variable. The predictor variables included cognitive function, metabolism in ANS-related brain regions, age, sex, and cardiovascular risk factors such as BMI, dyslipidemia, hypertension, and diabetes (Supplementary Table 9). In Model 1, both cognitive function and metabolism in the left hippocampus were identified as significant predictors of the QTc interval. In Models 2 and 3, cognitive function, metabolism in the bilateral caudate nucleus, and

age emerged as important predictors, while the other variables were not selected.

Interactions between CI and LV electrical instability

As shown in Supplementary Table 10, after adjusting for family history, serum albumin, brain natriuretic peptide (BNP), and CI, LV electrical instability (QTc interval) remained an independent risk factor for MAEs in HFrEF patients (HR_{adj}: 1.036 [95% CI: 1.007–1.066]; P=0.014). However, after correcting for family history, serum albumin, BNP, and QTc interval, CI was no longer an independent predictor of MAEs risk (HR_{adj}: 2.971 [95% CI:

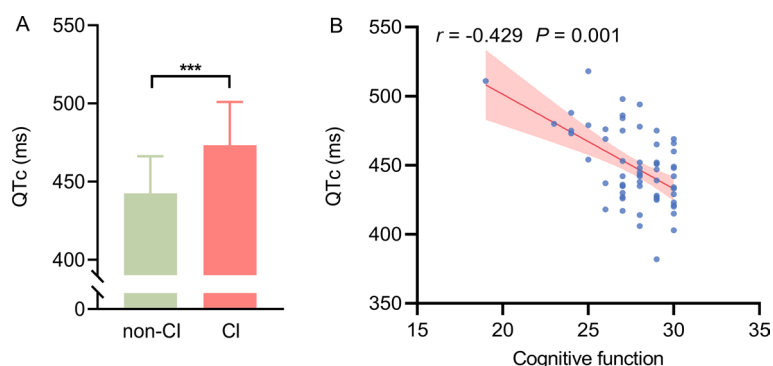


Fig. 3 Cognitive function and left ventricular electrical instability in patients with HFref. **A** Compared to patients without CI, the left ventricular electrical activity in HFref patients with CI was more disordered (QTc interval was prolonged); **B** Cognitive function was significantly related to QTc interval. CI=cognitive impairment; QTc=corrected QT interval

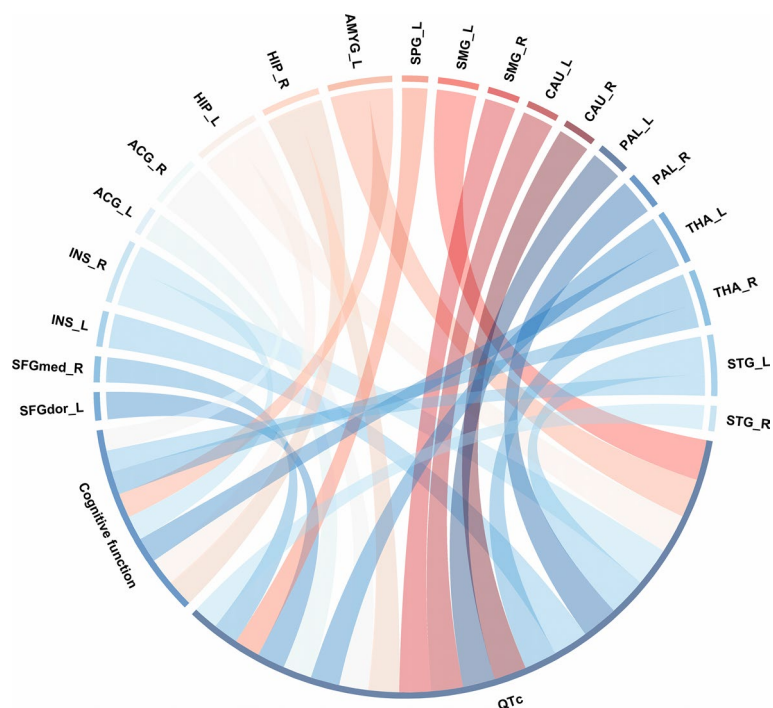


Fig. 4 Relationship between cognitive function, metabolism in ANS-related brain regions, and left ventricular electrical instability. Cognitive function and QTc interval were significantly correlated with part of the ANS-related brain regions metabolism. Band width indicates the number of correlations. ANS=autonomic nervous system; QTc=corrected QT. Abbreviations as in Fig. 2

0.751–11.744]; $P=0.121$). A risk reclassification analysis of MAEs was conducted to assess whether the incremental prognostic value of CI is related to the QTc interval. The NRI was calculated using four risk categories (0–20%, 20–40%, 40–60%, and >60%). When CI was added to the QTc interval, no reclassification was observed ($P=0.182$) (Supplementary Table 11). Additionally, there was a significant interaction between CI and QTc interval (HR_{adj} : 1.004 [95% CI: 1.001–1.007]; $P_{interaction}=0.014$).

Intermediary model analysis

We further investigated the effects of impaired metabolism in the left hippocampus and bilateral caudate nuclei on MAEs. Specifically, we assessed the effect of impaired CAN on MAEs in patients with CI by setting the QTc interval as the mediator. The QTc interval emerged as a mediator in the association between CAN and MAEs, accounting for 25.7%–40.8% of the total effects (all $p < 0.05$; Supplementary Fig. 5). After correcting for

cognitive function, the QTc interval served as a mediating factor for the association between the left hippocampus and MAE, accounting for 33.1% of the total effect ($p < 0.05$). Furthermore, LV electrical instability did not account for 100% of the total effect, suggesting that other mechanisms also link neural activity to MAEs.

Connectivity of CAN

Patients with CI exhibited reduced connectivity strength (low connectivity) in both the sympathetic and parasympathetic networks compared to patients without CI (Fig. 5). The sympathetic-related hypoconnectivity network between patients with and without CI consisted of 16 edges distributed over 14 nodes (all $p < 0.05$; FWE-corrected, 5000 permutations). These nodes included the bilateral dorsolateral prefrontal cortex, bilateral insula, bilateral anterior cingulate gyrus, bilateral middle cingulate gyrus, bilateral amygdala, right supramarginal gyrus, bilateral putamen, and left thalamus. The parasympathetic-related hypoconnective network between patients with and without CI consisted of nine edges distributed over 11 nodes (all $p < 0.05$; FWE-corrected, 5000 permutations). These nodes included the bilateral supplementary motor areas, bilateral hippocampus, bilateral amygdala, right supramarginal gyrus/angular gyrus, bilateral caudate nucleus, and left superior temporal gyrus/middle temporal gyrus.

Discussion

Main findings

This study provides unique insights into the intricate relationship among cognitive function, ANS-related neurometabolism, and prognosis in patients with HFrEF. Our findings revealed that patients with MAEs exhibited

significant cognitive deficits across various domains, and cognitive function emerged as an independent predictor of MAE risk in HFrEF. Additionally, patients with CI exhibited impaired ANS-related neurometabolism and LV electrical instability. Multivariate linear regression indicated a close relationship among these factors. However, Cox regression analysis showed that predictive value of cognitive function is not independent of QTc interval. Finally, the establishment of a metabolic brain network revealed reduced CAN connectivity in HFrEF patients with CI. Our results suggested that CI and ANS disorders are two clinical manifestations resulting from CAN damage. The increased risk of MAEs in HFrEF patients with CI may be attributed to impaired neurometabolism and connectivity of the CAN, leading to LV electrical instability (Central Illustration).

Potential mechanisms for the relationship between CI and MAEs

Previous studies have consistently shown that CI is prevalent in HF patients and significantly affects their prognosis [20, 36, 37]. Consistent with these findings, our present study revealed that HFrEF patients with CI had an elevated risk of MAEs or all-cause mortality. We observed that HFrEF patients with MAEs exhibited impaired cognitive function, particularly in orientation, registration, language, and praxis, compared to those without MAEs. This underscores the importance of cognitive function as a potential predictor of MAE risk. Notably, this study was the first to explore the relationship between cognitive function and MAE risk. However, poor compliance with medical treatment and self-care management hinders a full understanding of the mechanisms underlying poor prognoses.

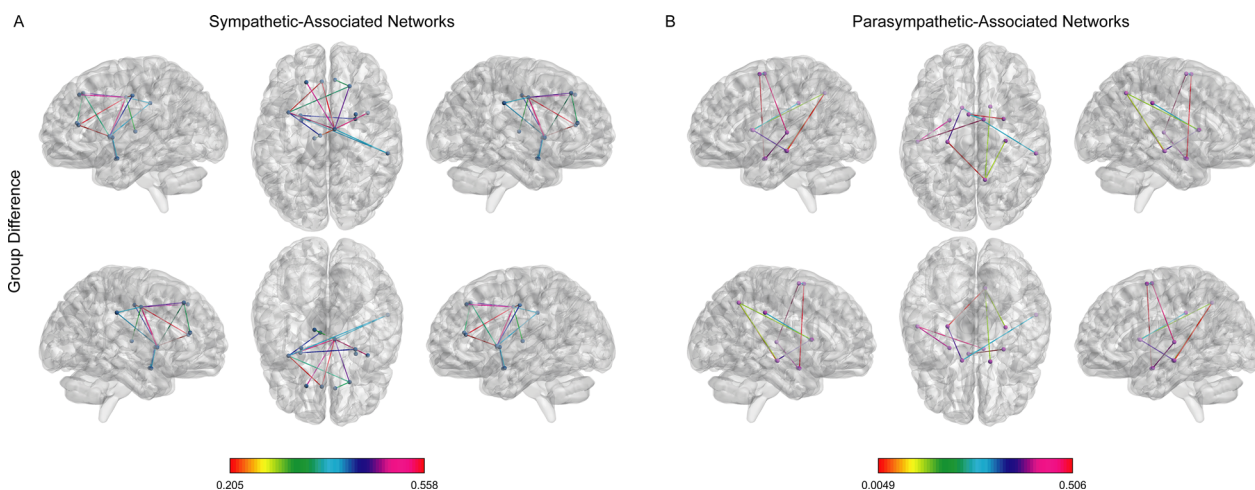


Fig. 5 Hypoconnectivity among the ANS-associated brain networks. Comparison of the **A** sympathetic- and **B** parasympathetic-associated brain networks between patients with and without CI (family-wise error corrected; $p < 0.05$). CI = cognitive impairment

Recent studies have indicated that individuals with CI often exhibit a prolonged QTc interval and altered heart rate variability [38–40]. These anomalies could stem from regional brain damage involved in the regulation of cardiac autonomic function [40, 41]. Our study's findings support this perspective, showing that HFrEF patients with CI exhibit impaired metabolic activity of ANS-associated brain regions (metabolism (left hippocampus and bilateral caudate nucleus) along with a prolonged QTc interval. The hippocampus is a crucial region of the limbic system that plays a vital role in spatial and episodic memory and is heavily involved in modulating the cardiac ANS [42–44]. Non-invasive measures of anatomical and functional connectivity in humans demonstrate a clear relationship between the caudate and executive frontal areas [45]. Furthermore, the caudate nucleus is a classical CAN region specific to sympathetic vagal control [17]. Unfortunately, the hippocampus and bilateral caudate nuclei are highly susceptible to hypoxia and hypoperfusion, both of which are common occurrences during HF progression. ANS-related neurometabolic impairments may lead to impaired cognitive function and ANS activity in patients with HF.

This study also revealed important correlations among cognitive function, QTc interval, and metabolism of ANS-related brain regions (including the insula, anterior cingulate gyrus, hippocampus, amygdala, caudate nucleus, thalamus, and superior temporal gyrus). Notably, Cox regression model analysis showed that the predictive value of cognitive function is not independent of the QTc interval and there is a significant interaction. These results highlight the overlapping central autonomic substrates associated with cognition and ANS responses. Subsequent mediation analyses further demonstrated that LV electrical instability due to ANS-related nerve injury is a primary factor contributing to the increased risk of MAEs in HFrEF patients with CI. Notably, our analysis revealed that variations in cognitive function could not be attributed to impaired LVEF, prevalent comorbidities, or biochemical markers.

Prognostic impact of CAN disorder in HFrEF patients with CI

Our findings revealed that HFrEF patients with CI exhibited a significant decrease in CAN connectivity, affecting both the sympathetic- and parasympathetic-related networks. The impairment in CAN connectivity was more pronounced in HFrEF patients with CI than in the compromised ANS-related neurometabolic activity. These findings highlighted the potential significance of CAN connectivity in these patients. Additionally, our findings indicated that the impaired ANS-related neurometabolism in HFrEF patients with CI is associated with

the nodes of the parasympathetic nerve-related network. This finding is consistent with prior research suggesting that the intricate central network regulating parasympathetic function at rest is disrupted in the early stages of Parkinson's disease [46]. Recent investigations have indicated that APOE4 carriers at risk for Alzheimer's disease exhibit impairments in higher-order ANS and parasympathetic activity [47]. This is consistent with our findings of impaired CAN functional connectivity and more severe parasympathetic-related neurometabolic impairments in HFrEF patients with CI. Another study reported that reduced functional connectivity between the amygdala and caudate nucleus predicted reduced post-induction heart rate variability in individuals with generalized anxiety disorder, highlighting the overlapping neural substrates associated with cognitive and ANS responses in patients with generalized anxiety disorder [48]. Our study also observed reduced functional connectivity between the amygdala and caudate nucleus, suggesting that parts of the CNS may be involved in both cognitive and ANS response processes.

These results suggested a significant association between CI and ANS dysfunction. In patients with ischemic HF, cellular excitability and connectivity impairment, combined with imbalanced sympathetic nerve innervation, heterogeneity of scar boundary conduction, fibrosis, and repolarization interaction, create favourable conditions for re-entrant arrhythmias [26, 49]. LV electrical instability may exacerbate with increased ANS activity, thereby increasing the risk of ventricular arrhythmia (VA) in patients with HF [26, 50]. Thus, these findings suggest that HFrEF patients with CI may experience reduced metabolism in ANS-related brain regions and diminished CAN connectivity, leading to peripheral ANS disorder and ultimately increasing repolarization dispersion and VA risk. This finding may support the pathophysiological mechanisms underlying the high prevalence of MAEs in HFrEF patients with CI.

Clinical implications

Our study adds to the growing evidence for the integration of cognitive and ANS regulation by shared central autonomic mechanisms. Importantly, our findings indicate that adverse outcomes in HFrEF patients with CI are largely attributable to the exacerbation of LV electrical instability resulting from ANS disorder, which are associated with reduced metabolism in ANS-related brain regions and CAN connectivity. This research avenue holds promise in advancing our understanding of cognitive assessment methods and their implications for cardiovascular health. This study emphasizes the importance of preliminary screening of patients in the high-risk groups for MAEs and early intervention through a simple

cognitive scale assessment during clinical practice. In addition, we proposed that targeted intervention in CAN (including physical exercise, transcranial magnetic stimulation, and direct current stimulation) is potentially effective in improving cognitive function and ANS flexibility in patients with HF.

Study limitations

This study was a single-centre, small-sample, observational investigation. Therefore, the findings may not be generalizable, and larger prospective studies at different centres are needed to confirm these findings. In clinical practice, both the Montreal Cognitive Assessment and MMSE are used for cognitive assessment, although the MMSE may not adequately capture mild cognitive issues. Further research is required to explore the associations among various cognitive tests, ANS dysfunction, and adverse outcomes. However, considering the clinical factors, the MMSE seems more suitable for clinical practice. Moreover, longitudinal monitoring of alternation in cognitive impairment in patients with HF could provide a deeper understanding of the connection between CI and MAEs. Although the mediation analysis suggests a causal effect, it does not establish causation. Hence, future studies should employ long-term imaging techniques to observe dynamic changes in cognitive function, ANS, and adverse prognosis. Finally, advanced scanning techniques such as PET/MRI offer insights into the complex interactions between the heart and brain in patients with HFrEF.

Conclusions

Our study revealed that CI and ANS disorders are two clinical manifestations resulting from CAN damage. Additionally, impaired in specific brain regions and network connectivity within the CAN contributed to LV electrical instability and subsequent MAEs, which represents one of the main mechanisms underlying poor prognosis of HFrEF patients with CI. This interaction provides novel insights into the adverse outcomes observed in HFrEF patients with CI. Further comprehensive studies are necessary to validate these findings.

Abbreviations

AAL	Automated anatomical labeling
ANS	Autonomic nervous system
BMI	Body mass index
BNP	Brain natriuretic peptide
BW	Bandwidth
CAN	Central autonomic network
CI	Cognitive impairment
CT	Computed tomography
FDG	¹⁸ F-fluorodeoxyglucose
GMPI	Gated myocardial perfusion imaging
LV	Left ventricular
LVEF	Left ventricular ejection fraction
HF	Heart failure

HFrEF	Heart failure with reduced ejection fraction
HR	Hazard ratios
HR _{adj}	Adjusted hazard ratio
IQR	Interquartile range
MAEs	Major arrhythmic events
MMSE	Mini-mental state examination
MNI	Montreal neurological institute
NRI	Net reclassification improvement
PET	Positron emission tomography
QTc	Heart rate-corrected QT
SD	Standard deviation
SPECT	Single-photon emission computed tomography
SUV _{mean}	Standardized uptake values (mean)
TPD	Total perfusion deficit
VA	Ventricular arrhythmia

Supplementary Information

The online version contains supplementary material available at <https://doi.org/10.1186/s13550-024-01183-6>.

Additional file 1.

Acknowledgements

The authors thank all their colleagues at the Department of Nuclear Medicine, Anzhen Hospital.

Author contributions

All authors were involved in study conception and design. ZYS and MKY prepared the materials and collected data. ZYS, BBN, EJZ, WF, and MKY were responsible for data analysis and interpretation. ZYS conducted the imaging studies and wrote the first draft of this manuscript. XLZ provided supervision. ZYS, SJL, WF, BCS, XL, MKY, and XLZ contributed to the discussion. XLZ, MKY, SJL, and XL critically revised the manuscript. All authors reviewed previous manuscript versions and approved the final version for submission.

Funding

This work was supported by the National Natural Science Foundation of China (82171994, 81871377, and 82027804), Beijing Municipal Administration of Hospitals (ZYLX202110), and the Advanced Research Foundation of Capital Medical University (PYZ21121).

Data availability

The data supporting the findings of this study are available from the corresponding author upon reasonable request.

Declarations

Competing Interests

The authors report no relationships relevant to the contents of this paper.

Ethics approval and consent to participate

The study protocol was approved by the Ethics Committee of the Beijing Anzhen Hospital of Capital Medical University (No. 2017024) and adhered to the principles of the Declaration of Helsinki. Written informed consent was obtained from all the participants.

Consent for publication

Written informed consent was obtained from the patients for publication of this study and accompanying images.

Author details

¹Department of Nuclear Medicine, Molecular Imaging Lab, Beijing Anzhen Hospital, Capital Medical University, Beijing, China. ²Division of Nuclear Technology and Applications, Institute of High Energy Physics, Chinese Academy of Sciences, Beijing, China. ³Department of Cardiac Surgery, Beijing Anzhen Hospital, Capital Medical University, Beijing, China. ⁴Department of Nuclear Medicine, First Hospital of Shanxi Medical University, Taiyuan, Shanxi, China. ⁵Division of Nuclear Medicine, Department of Biomedical Imaging

and Image-Guided Therapy, Medical University of Vienna, Vienna, Austria.
⁶Department of Nuclear Medicine, Beijing Chest Hospital, Capital Medical University & Beijing Tuberculosis and Tumour Research Institute, Beijing, China.

Received: 2 August 2024 Accepted: 18 November 2024
 Published online: 28 November 2024

References

- Rosignol P, Hernandez AF, Solomon SD, Zannad F. Heart failure drug treatment. *The Lancet*. 2019;393(10175):1034–44.
- Riganello F, Vatrano M, Tonin P, Cerasa A, Cortese MD. Heart rate complexity and autonomic modulation are associated with psychological response inhibition in healthy subjects. *Entropy*. 2023. <https://doi.org/10.3390/e25010152>.
- Nonogaki Z, Umegaki H, Makino T, Suzuki Y, Kuzuya M. Relationship between cardiac autonomic function and cognitive function in Alzheimer's disease. *Geriatr Gerontol Int*. 2017;17:92–8. <https://doi.org/10.1111/ggi.12679>.
- Hu G, Collet JP, Zhao M, Lu Y, Wang Y. Associations between autonomic function and cognitive performance among patients with cerebral small vessel disease. *Brain Sci*. 2023. <https://doi.org/10.3390/brainsci13020344>.
- Chou YT, Sun ZJ, Shao SC, Yang YC, Lu FH, Chang CJ, et al. Autonomic modulation and the risk of dementia in a middle-aged cohort: a 17-year follow-up study. *Biomed J*. 2023;46: 100576. <https://doi.org/10.1016/j.bj.2022.12.004>.
- Chen CW, Kwok YT, Cheng YT, Huang YS, Kuo TBJ, Wu CH, et al. Reduced slow-wave activity and autonomic dysfunction during sleep precede cognitive deficits in Alzheimer's disease transgenic mice. *Sci Rep*. 2023;13:11231. <https://doi.org/10.1038/s41598-023-38214-6>.
- Goyal P, Didomenico RJ, Pressler SJ, Ibeh C, White-Williams C, Allen LA, et al. Cognitive impairment in heart failure: a heart failure society of america scientific statement. *J Card Fail*. 2024;30:488–504. <https://doi.org/10.1016/j.cardfail.2024.01.003>.
- Wu Y, Chen L, Zhong F, Zhou K, Lu C, Cheng X, et al. Cognitive impairment in patients with heart failure: molecular mechanism and therapy. *Heart Fail Rev*. 2023;28:807–20. <https://doi.org/10.1007/s10741-022-10289-9>.
- Stavakis S, Kulkarni K, Singh JP, Katrasis DG, Aroundas AA. Autonomic modulation of cardiac arrhythmias: methods to assess treatment and outcomes. *JACC Clin Electrophysiol*. 2020;6:467–83. <https://doi.org/10.1016/j.jacep.2020.02.014>.
- Benarroch EJ. The central autonomic network: functional organization, dysfunction, and perspective. 1993 68:988–1001. [https://doi.org/10.1016/s0025-6196\(12\)62272-1](https://doi.org/10.1016/s0025-6196(12)62272-1).
- Giudicessi JR, Noseworthy PA, Ackerman MJ. The QT interval. *Circulation*. 2019;139:2711–3. <https://doi.org/10.1161/CIRCULATIONAHA.119.039598>.
- Nicolini P, Lucchi T, Vicenzi M. Heart rate variability as a predictor of cognitive decline: a possible role for the central autonomic network. *Biomed J*. 2024;47: 100700. <https://doi.org/10.1016/j.bj.2024.100700>.
- Nicolini P, Lucchi T, Abbate C, Inglese S, Tomasini E, Mari D, et al. Autonomic function predicts cognitive decline in mild cognitive impairment: evidence from power spectral analysis of heart rate variability in a longitudinal study. *Front Aging Neurosci*. 2022;14: 886023. <https://doi.org/10.3389/fnagi.2022.886023>.
- Thayer JF, Lane RD. A model of neurovisceral integration in emotion regulation and dysregulation. *J Affect Dis*. 2000;61(3):201–16.
- Thayer JF, Hansen AL, Saus-Rose E, Johnsen BH. Heart rate variability, prefrontal neural function, and cognitive performance: the neurovisceral integration perspective on self-regulation, adaptation, and health. *Ann Behav Med*. 2009;37:141–53. <https://doi.org/10.1007/s12160-009-9101-z>.
- E E B, F L C. Central autonomic disorders. 1993;10. <https://doi.org/10.1097/00004691-199301000-00005>.
- Beissner F, Meissner K, Bar KJ, Napadow V. The autonomic brain: an activation likelihood estimation meta-analysis for central processing of autonomic function. *J Neurosci*. 2013;33:10503–11. <https://doi.org/10.1523/JNEUROSCI.1103-13.2013>.
- Lin F, Ren P, Wang X, Anthony M, Tadin D, Heffner KL. Cortical thickness is associated with altered autonomic function in cognitively impaired and non-impaired older adults. *J Physiol*. 2017;595:6969–78. <https://doi.org/10.1111/JP274714>.
- Critchley HD. Neural mechanisms of autonomic, affective, and cognitive integration. *J Comp Neurol*. 2005;493:154–66. <https://doi.org/10.1002/cne.20749>.
- Almeida OP, Garrido GJ, Beer C, Lautenschlager NT, Arnolda L, Flicker L. Cognitive and brain changes associated with ischaemic heart disease and heart failure. *Eur Heart J*. 2012;33:1769–76. <https://doi.org/10.1093/eurheartj/ehr467>.
- Frey A, Homola GA, Henneges C, Muhlbauer L, Sell R, Kraft P, et al. Temporal changes in total and hippocampal brain volume and cognitive function in patients with chronic heart failure—the COGNITION. MATTERS-HF cohort study. *Eur Heart J*. 2021;42:1569–78. <https://doi.org/10.1093/eurheartj/ehab003>.
- Woo MA, Macey PM, Fonarow GC, Hamilton MA, Harper RM. Regional brain gray matter loss in heart failure. *J Appl Physiol*. 2003;95(2):677–84.
- Zhong S, Ding W, Sun L, Lu Y, Dong H, Fan X, et al. Decoding the development of the human hippocampus. *Nature*. 2020;577:531–6. <https://doi.org/10.1038/s41586-019-1917-5>.
- Papez JW. A proposed mechanism of emotion. 1937. *J Neuropsychiatry Clin Neurosci*. 1995;7(1):103–12.
- Bai Y, Yun M, Nie B, Shan L, Liu W, Hacker M, et al. Neurometabolism and ventricular dyssynchrony in patients with heart failure and reduced ejection fraction. *J Am Coll Cardiol*. 2022;80:1884–96. <https://doi.org/10.1016/j.jacc.2022.08.801>.
- Donahue JK, Chrispin J, Ajjola OA. Mechanism of ventricular tachycardia occurring in chronic myocardial infarction scar. *Circ Res*. 2024;134:328–42. <https://doi.org/10.1161/CIRCRESAHA.123.321553>.
- Brück A, Virta JR, Koivunen J, Koikkalainen J, Scheinin NM, Helenius H, Rinne JO. [11 C] PIB, [18 F] FDG and MR imaging in patients with mild cognitive impairment. *European J Nucl Med Mol Imag*. 2013;40:1567–72.
- Meyer P, Frings L, Rücker G. Hellwig S. Society of nuclear medicine. F-FDG PET Parkinsonism Differ Diagn Eval Cognit Impair. 2017;58:1888–98. <https://doi.org/10.2967/jnumed.116.186403>.
- Ponikowski P, Voors AA, Anker SD, Bueno H, Cleland JG, Coats AJ, et al. ESC Guidelines for the diagnosis and treatment of acute and chronic heart failure: the task force for the diagnosis and treatment of acute and chronic heart failure of the European society of cardiology (ESC). Developed with the special contribution of the heart failure association (HFA) of the ESC. *Eur J Heart Fail*. 2016;18:891–975. <https://doi.org/10.1002/ejhf.592>.
- Yun M, Nie B, Wen W, Zhu Z, Liu H, Nie S, et al. Assessment of cerebral glucose metabolism in patients with heart failure by (18)F-FDG PET/CT imaging. *J Nucl Cardiol*. 2022;29:476–88. <https://doi.org/10.1007/s12350-020-02258-2>.
- Cho SG, Jabin Z, Park KS, Kim J, Kang SR, Kwon SY, Bom HS. Clinical values of left ventricular mechanical dyssynchrony assessment by gated myocardial perfusion SPECT in patients with acute myocardial infarction and multivessel disease. *European J Nucl Med Mol Imag*. 2017;44:259–66.
- Dilsizian V, Bacharach SL, Beanlands RS, Bergmann SR, Delbeke D, Dorbala S, et al. ASNC imaging guidelines/SNMMI procedure standard for positron emission tomography (PET) nuclear cardiology procedures. *J Nucl Cardiol*. 2016;23:1187–226. <https://doi.org/10.1007/s12350-016-0522-3>.
- Zhang X, Liu XJ, Hu S, Schindler TH, Tian Y, He ZX, Schelbert HR. Long-term survival of patients with viable and nonviable aneurysms assessed by 99mTc-MIBI SPECT and 18F-FDG PET: a comparative study of medical and surgical treatment. *J Nucl Med*. 2008;49(8):1288–98.
- Varrone A, Asenbaum S, Vander Borcht T, Booi J, Nobili F, Nagren K, et al. EANM procedure guidelines for PET brain imaging using [18F]FDG, version 2. *Eur J Nucl Med Mol Imaging*. 2009;36:2103–10. <https://doi.org/10.1007/s00259-009-1264-0>.
- Templin C, Hanggi J, Klein C, Topka MS, Hiestand T, Levinson RA, et al. Altered limbic and autonomic processing supports brain-heart axis in Takotsubo syndrome. *Eur Heart J*. 2019;40:1183–7. <https://doi.org/10.1093/eurheartj/ehz068>.
- Holm H, Bachus E, Jujic A, Nilsson ED, Wadstrom B, Molvin J, et al. Cognitive test results are associated with mortality and rehospitalization in heart failure: Swedish prospective cohort study. *ESC Heart Fail*. 2020;7:2948–55. <https://doi.org/10.1002/ehf2.12909>.
- Taylor J. Cognitive impairment predicts worse outcome in heart failure. *European Heart J*. 2015;36(30):1945–1945.

38. Terroba-Chambi C, Bruno V, Vigo DE, Merello M. Heart rate variability and falls in Huntington's disease. *Clin Auton Res*. 2021;31:281–92. <https://doi.org/10.1007/s10286-020-00669-2>.
39. Zulli R, Nicosia F, Borroni B, Agosti C, Prometti P, Donati P, et al. QT dispersion and heart rate variability abnormalities in Alzheimer's disease and in mild cognitive impairment. *J Am Geriatr Soc*. 2005;53:2135–9. <https://doi.org/10.1111/j.1532-5415.2005.00508.x>.
40. Danese A, Federico A, Martini A, Mantovani E, Zucchella C, Tagliapietra M, et al. QTc prolongation in patients with dementia and mild cognitive impairment: neuropsychological and brain imaging correlations. *J Alzheimers Dis*. 2019;72:1241–9. <https://doi.org/10.3233/JAD-190632>.
41. Toledo MA, Junqueira LF Jr. Cardiac autonomic modulation and cognitive status in Alzheimer's disease. *Clin Auton Res*. 2010;20:11–7. <https://doi.org/10.1007/s10286-009-0035-0>.
42. Dimsdale-Zucker HR, Ritchey M, Ekstrom AD, Yonelinas AP, Ranganath C. CA1 and CA3 differentially support spontaneous retrieval of episodic contexts within human hippocampal subfields. *Nat Commun*. 2018;9:294. <https://doi.org/10.1038/s41467-017-02752-1>.
43. Torromino G, Autore L, Khalil V, Mastrorilli V, Griguoli M, Pignataro A, et al. Offline ventral subiculum-ventral striatum serial communication is required for spatial memory consolidation. *Nat Commun*. 2019;10:5721. <https://doi.org/10.1038/s41467-019-13703-3>.
44. Santini CO, Fassini A, Scopinho AA, Busnardo C, Correa FM, Resstel LB. The ventral hippocampus NMDA receptor/nitric oxide/guanylate cyclase pathway modulates cardiovascular responses in rats. *Auton Neurosci*. 2013;177:244–52. <https://doi.org/10.1016/j.autneu.2013.05.008>.
45. Grahm JA, Parkinson JA, Owen AM. The cognitive functions of the caudate nucleus. *Prog Neurobiol*. 2008;86:141–55. <https://doi.org/10.1016/j.pneur.2008.09.004>.
46. Tessa C, Toschi N, Orsolini S, Valenza G, Lucetti C, Barbieri R, et al. Central modulation of parasympathetic outflow is impaired in de novo Parkinson's disease patients. *PLoS ONE*. 2019;14: e0210324. <https://doi.org/10.1371/journal.pone.0210324>.
47. Lohman T, Kapoor A, Engstrom AC, Shenasa F, Alitin JPM, Gaubert A, et al. Central autonomic network dysfunction and plasma Alzheimer's disease biomarkers in older adults. *Alzheimers Res Ther*. 2024;16:124. <https://doi.org/10.1186/s13195-024-01486-9>.
48. Makovac E, Meeten F, Watson DR, Herman A, Garfinkel SN, DC H, et al. Alterations in amygdala-prefrontal functional connectivity account for excessive worry and autonomic dysregulation in generalized anxiety disorder. *Biol Psychiatry*. 2016;80:786–95. <https://doi.org/10.1016/j.biopsych.2015.10.013>.
49. Abd-Elmoniem KZ, Tomas MS, Sasano T, Soleimanifard S, Vonken EJP, Youssef A, Abraham MR. Assessment of distribution and evolution of mechanical dyssynchrony in a porcine model of myocardial infarction by cardiovascular magnetic resonance. *J Cardiovasc Magn Resonan*. 2012;14(1):1.
50. Chatterjee NA, Singh JP. Autonomic modulation and cardiac arrhythmias: old insights and novel strategies. *Europace*. 2021;23:1708–21. <https://doi.org/10.1093/europace/euab118>.

Publisher's Note

Springer Nature remains neutral with regard to jurisdictional claims in published maps and institutional affiliations.